

Winter Classification of Mandibular Impacted Third Molars Based on Convolutional Neural Networks

Mandibular Gömülü Üçüncü Molar Dişlerin Evrişimsel Sinir Ağlarına Dayalı Winter Sınıflaması

Mustafa Taha GÜLLER¹

¹Department of Oral, Dental and Maxillofacial Radiology, Giresun University, Faculty of Dentistry, Giresun, Türkiye



Nida KUMBASAR²

²TUBİTAK, Informatics and Information Security Research Center (BİLGEM), Kocaeli, Türkiye



Özkan MİLOĞLU³

³Department of Oral, Dental and Maxillofacial Radiology, Atatürk University, Faculty of Dentistry, Erzurum, Türkiye



İbrahim Yücel ÖZBEK⁴

⁴Department of Electrical Electronic Engineering (High Performance Comp Applicat & Res Ctr), Atatürk University, Erzurum, Türkiye



Emin Argün ORAL⁴

⁴Department of Electrical Electronic Engineering (High Performance Comp Applicat & Res Ctr), Atatürk University, Erzurum, Türkiye



Geliş Tarihi/Received 23.05.2024
Revizyon Talebi/Revision Requested 16.09.2024
Son Revizyon/Last Revision 25.09.2024
Kabul Tarihi/Accepted 07.02.2025
Yayın Tarihi/Publication Date 25.02.2026

Sorumlu Yazar/Corresponding author:

Mustafa Taha GÜLLER
E-mail: dt.mtguller@gmail.com

Cite this article: Güller MT, Kumbasar N, Miloğlu Ö, Özbek İY, Oral EA. Winter Classification of Mandibular Impacted Third Molars Based on Convolutional Neural Networks. *Curr Res Dent Sci.* 2026; 36(2): 133-139 / doi:10.17567/currendentsci.1488041



Content of this journal is licensed under a Creative Commons Attribution-NonCommercial-NoDerivatives 4.0 International License

ABSTRACT

Objective: Winter classification (WC) is used in the radiographic evaluation of mandibular impacted third molars (MITM) before extraction. In our study, we investigated the classification performance of panoramic radiographs (PRs) using different versions of two convolutional networks (CNN).

Methods: The analysis was performed using three different YOLO-v7 and five different YOLO-v8 CNN architectures for the WC of 716 MITM teeth in 532 PRs included in the dataset. The localization of the second and third molars on PR images was determined, and the diagnostic performance of WC in this area was measured. Precision, recall, and mean average precision (mAP) were statistically evaluated for each model.

Results: For both architectures, the highest performance was obtained for horizontal classification, with a value of 0.917 for the mAP metric, while the lowest performance was found to be 0.799 for vertical classification. Looking at the mAP metric values for all classes in the study, YOLO-v8-m performed better than YOLO-v7, with a difference of 2.7%, resulting in an overall mAP of 0.838 for YOLO-v7 and 0.865 for YOLO-v8. For both YOLO-v7 and YOLO-v8, the mid-depth network performed better than the other sub-models.

Conclusions: This is the first study in which WC is performed using YOLO-v7 and YOLO-v8 models. In line with our results, CNN models for WC in PR are promising. In future studies, better results can be obtained by increasing the dataset size, using images from different centers and developing CNN architectures. Thus, clinical use of artificial intelligence architectures may become widespread.

Keywords: Convolutional neural network, object detection, panoramic radiography, third molar, winter classification

ÖZ

Amaç: Winter sınıflaması (WC), gömülü mandibular üçüncü molar dişlerin (MITM) çekim öncesi radyografik değerlendirmesinde kullanılır. Çalışmamızda iki evrişimli sinir ağının (CNN) farklı versiyonlarını kullanarak panoramik radyografilerde (PR) sınıflandırma performansını araştırdık.

Yöntemler: Veri setini oluşturan 532 panoramik radyografideki (PR) 716 MITM dişin WC'si, üç farklı YOLO-v7 ve beş farklı YOLO-v8 CNN mimarisi kullanılarak analiz edildi. PR görüntülerinde ikinci ve üçüncü molarların lokalizasyonu belirlendi ve bu bölgedeki WC'nin tanılabilir performansı ölçüldü. Kesinlik, geri çağırma ve genel ortalama kesinlik (mAP) her model için istatistiksel olarak değerlendirildi.

Bulgular: Her iki mimari için en yüksek performans, 0,917 mAP değeri ile yatay sınıflandırma için elde edilirken, en düşük performans dikey sınıflandırmada 0,799 olarak bulunmuştur. Çalışmadaki tüm sınıflar için mAP değerlerine bakıldığında, YOLO-v8-m, YOLO-v7'den %2,7 daha iyi performans göstermiş ve YOLO-v7 için 0,838 ve YOLO-v8 için 0,865 mAP değeri elde edilmiştir. Hem YOLO-v7 hem de YOLO-v8 için, orta derinlikteki ağ diğer alt modellerden daha iyi performans göstermektedir.

Sonuç: Bu çalışma, YOLO-v7 ve YOLO-v8 modelleri kullanılarak WC'nin gerçekleştirildiği ilk çalışmadır. Sonuçlarımızla uyumlu olarak, PR'de WC için kullanılan CNN modelleri umut vericidir. Gelecek çalışmalarda veri sayısını artırarak, farklı merkezlerden görüntüler kullanarak ve CNN mimarilerini geliştirerek daha iyi sonuçlar elde edilebilir. Böylece yapay zeka mimarilerinin klinik kullanımı yaygınlaşabilir.

Anahtar Kelimeler: Evrişimli sinir ağı, nesne algılama, panoramik radyografi, üçüncü molar, winter sınıflaması

INTRODUCTION

Teeth can remain impacted for various local or systemic reasons, including genetic disorders, adjacent teeth, alveolar bone, surrounding soft tissue, trauma, systemic diseases, lesions in the jaw, and the tooth's position.^{1,2} Mandibular impacted third molars (MITM) are the most commonly impacted teeth.³ Conditions such as pain, caries, infection, root resorption, periodontal disease, cysts, or tumors in the impacted tooth are common indications for extraction.^{3,4}

Impacted teeth should be examined before extraction, and the appropriate surgical procedure should be determined. Panoramic radiographs (PRs) are often used in the radiological examination performed for this purpose. In the preoperative PRs, certain classifications of the impacted tooth are made. In the Winter classification (WC), which is used to classify MITM teeth, the angulation of the tooth relative to the second molar is considered.⁵

The use of artificial intelligence (AI) for diagnosis and treatment planning in the medical field is increasing. In dentistry, studies are being conducted in areas such as oral radiology and pathology, endodontics, restorative dentistry, periodontics, and orthodontics.⁶⁻¹⁰ AI models primarily focus on image analysis due to the large amount of radiological data and the widespread use of radiographs for diagnosis.

In the literature, only a limited number of studies have used AI to perform WC on MITM teeth.¹¹⁻¹⁴ While one study examined only two classes (horizontal and mesioangular),¹¹ others used only a convolutional neural network model.¹²⁻¹⁴ No study has comparatively analysed WC using two neural network models, nor has YOLO-v8, a current convolutional neural network model, been used. This study aims to automatically perform WC on PRs using a total of eight different versions of two deep learning models (YOLO-v7 and YOLO-v8) and to compare the performance of their architectures.

METHODS

In this section, we first explain the dataset collected for WC and its preprocessing, followed by the increase of the dataset. The second section describes how the WC is performed. In the third section, the labelling of the dataset and, in the last section, we mention the CNN algorithms used for classification and the methods used to evaluate the datasets.

Data set

The study protocol was conducted in accordance with the tenets of the Declaration of Helsinki (Atatürk University Faculty of Dentistry Ethics Committee, Number: 04 / Date: January 20, 2021). Our study reviewed the radiological archive of Atatürk University Faculty of Dentistry, Department of Oral and Maxillofacial Radiology, between 2018 and 2022. PRs with unilateral or bilateral MITM were downloaded in bitmap format. If the root formation was incomplete or the crown was damaged, the adjacent second molar was missing or impacted, and artefacts on radiographic image, the PRs in question were excluded from the study. As a result, 532 PRs were included in the study.

PR images with a resolution of approximately 2957 x 1435 pixels were divided vertically from the centreline, and evaluated as the left side by taking the symmetry of the right side to increase the number of PRs and improve the performance of our model. A total of 716 MITM tooth records were generated.

Determination of WC identification of MITM

The WC is determined based on the angle between the third molar and the long axis of the second molar. An angle between 10° and -10° is classified as vertical, an angle between 11° and 79° is classified as mesioangular, an angle between -11° and -79° is classified as distoangular, an angle between 80° and 100° is classified as horizontal, and an angle between 111° and -80° is classified as other (buccolingual, inverted).⁴ In our study, 716 MITM teeth were examined in 4 classes (vertical, mesioangular, distoangular, and horizontal) (Figure 1). In this study, WC was determined on PR images by a researcher with five years of experience in oral and maxillofacial radiology. The online protractor tool (https://www.ginifab.com/feeds/angle_measurement/) was used to calculate the angle between the long axes of the 2nd and 3rd molars (Figure 2).

Labelling data for AI

PR images with a resolution of approximately 1500 x 700 pixels were labelled using the Labellmg¹⁵ tool to identify the 2nd and 3rd molars (Figure 3).

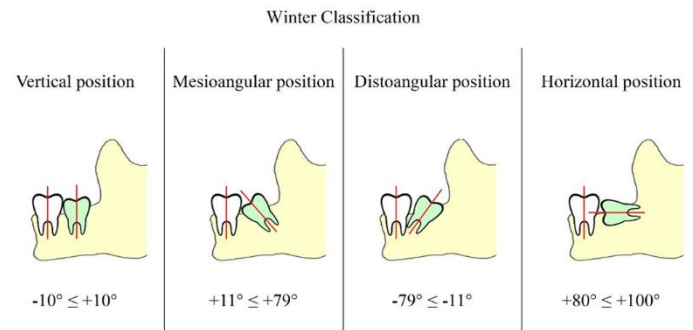


Figure 1. Winter classification

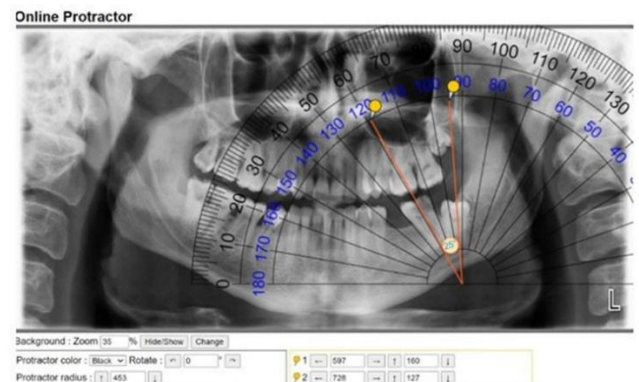


Figure 2. Measurement with the Online Protractor tool

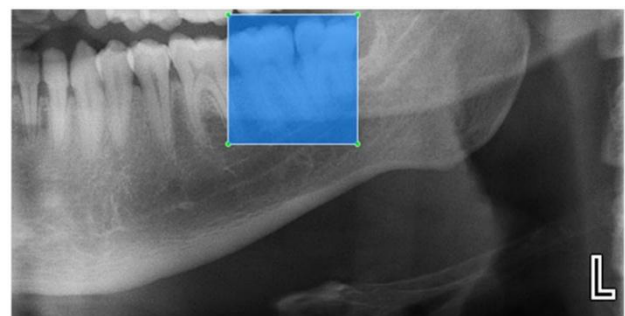


Figure 3. Labelling using Labellmg

WC model

In the object detection, it is determined which class the object belongs to and where it is located in the image. Recently, thanks to Convolutional Neural Networks (CNN) based deep architectures, the learning ability of AI has improved, and object detection has become increasingly popular. Compared to classical methods, hierarchical architectures with deeper layers for feature extraction have significantly improved the success of object detection in various applications. Object detection approaches are generally divided in two frameworks: one stage and two stage detectors. The first approach involves a region proposal at the preliminary stage, while the second directly determines the class and location without a region proposal.

YOLO (You Only Look Once) is a one stage object detector based on feature extraction and learning using a deep CNN architecture. The YOLO series, first proposed by Redmon et al.¹⁶, has become widely used in AI due to its speed and performance, particularly in object recognition problems. The YOLO framework consists of three key components: the head, neck, and spine, has been associated with various component sets and architectures. Several versions of YOLO have been introduced in the literature.¹⁷ The performance of the YOLO series has steadily improved with each new release performance.¹⁸ YOLO-v7, one of the most advanced versions of the series, achieves highly accurate results through the use of the Extended Efficient Layer Aggregation Networks module (E-ELAN), new model scaling, and auxiliary heads, which positively impact the speed/power ratio.¹⁹ Ultralytics proposed the state-of-the-art for YOLO-v8 by replacing all C3 builds in Yolo-v5 with builds that specify different channels for different scaling models, adding more hop connections and split operations.^{20,21} When tested on the COCO dataset,²² the mean average precision (mAP) value of the YOLO-v8 algorithm is shown significantly improved compared to other YOLO algorithms.²⁰

In this study, the versions of YOLO-v7 and YOLO-v8, which are popular methods for object recognition that provide both object location and class information, are comparatively analysed with different network depth and number of parameters. Within the scope of the study, eight submodels (YOLO-v7-tiny, YOLO-v7, YOLO-v7-x, YOLO-v8-n, YOLO-v8-s, YOLO-v8-m, YOLO-v8-l, YOLO-v8-x) with varying depths were trained separately for the WC problem and compared. Finally, using the bounding box containing 2nd and 3rd molars, the location of the teeth is determined, and the type of relationship between these two teeth is identified according to WC criteria.

Data set and model parameters

716 MITM dental images were randomly divided into three groups: 486 training (~68%), 114 validation (~16%) and 116 test (~16%) groups.

The images were resized to 640x640 before being input to the model. Data augmentation techniques were used during model training by changing the contrast of images, modifying the rotation angles, and creating mosaic patterns from different images. The experiments were repeated many times by changing the parameters. The highest performance was achieved using the SGD optimization algorithm with 150 epochs and a learning rate of 0.01. The batch size was set to 8 for YOLO-v7 models and 16 for YOLO-v8 models.

Evaluation metrics

In object detection problems, models predict the bounding box coordinates and the class of objects in the input images. In recent years, the average precision (AP) metric, widely used for object detection evaluation and specifically calculated for each object category, has been defined as the average detection sensitivity across different recall levels. The mAP is used as a metric to compare the performance across all object categories and provides an overall evaluation of the object recognition task by category.²³

Intersection over union (IoU) gives the overlap ratio between the boxes defined by the actual coordinates and the estimated coordinates (Equation 1). A threshold value is determined for metrics to be calculated. The relationship between IoU metric and threshold value in object detection problems is shown in Figure 4. True Positive (TP) refers to the correct detection of the ground truth bounding box, while False Positive (FP) refers to the incorrect detection of a non-existent object or the detection of a present object with an intersection ratio below the threshold. False Negative (FN) refers to the ground truth bounding box that is normally present but not detected. The IoU threshold value is generally taken as 0.5.

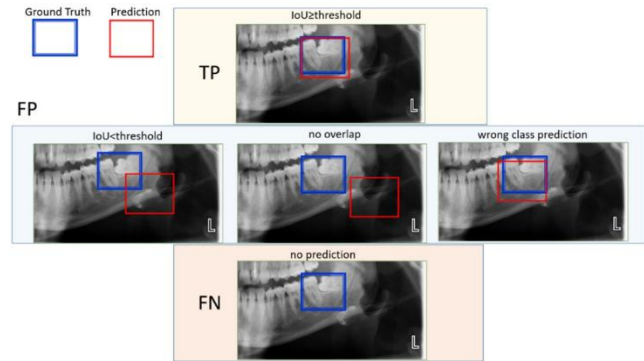


Figure 4. Representative image of True Positive (TP), False Positive (FP), False Negative (FN)

Precision (Equation 2) indicates how accurate the model is in identifying predicted objects, while Recall (Equation 3) refers to the model's ability to correctly detect all real objects. In model comparisons for object detection, high precision and recall values positively impact model performance. AP refers to the area under the precision-recall curve, evaluated at an specific IoU threshold (Equation 4). In object detection problems, it is calculated separately for each class. mAP represents the mean Average Precision for n classes in the problem (Equation 5).

In this study, the threshold for the IoU between the predicted and target frames was set to a value greater than 0.5. Precision and Recall metrics are also presented for detailed model-based and class-based analysis. This mAP metric was used to measure the models overall performance.

RESULTS

The current study included 716 MITM teeth: 182 vertical, 257 mesioangular, 172 distoangular, and 105 horizontally angled, belonging to 532 PRs (Table 1). The analysis of YOLO-v7 (YOLO-v7-tiny, YOLO-v7, YOLO-v7-x) and YOLO-v8 (YOLO-v8-n, YOLO-v8-s, YOLO-v8-m, YOLO-v8-l, YOLO-v8-x) experimental studies with different performance metrics, model depth parameters and test data inference time for all classes is presented (Table 2 and Table 3). As the layers in the models increase, the number of parameters and the GFLOP value, a measure of the computational speed equal to one billion floating point operations per second also increase. Figure 5 shows the general performance of the YOLO-v7 and YOLO-v8 models across all classes for the test data, based on the mAP value (mAP@50) at a threshold of 0.5 IoU. YOLO-v8-m performed the best among all models with a score of 0.865. For both YOLO-v7 and YOLO-v8, the mid-depth network performed better than the other sub-models.

When Figure 6 is analysed, the highest test data AP performance for the YOLO-v7 and YOLO-v8-m models among the four classes is found in the horizontal class. The mAP performance is 0.911 for YOLO-v7 and 0.917 for YOLO-v8, which are very close to each other. The lowest performance was observed in the vertical class, with 0.711 for YOLO-v7 and 0.799 for YOLO-v8-m.

Table 1. Number of impacted mandibular third molars belonging to winter class

| Winter class | Number of mandibular impacted third molar |
|--------------|---|
| Vertical | 182 |
| Mesioangular | 257 |
| Distoangular | 172 |
| Horizontal | 105 |
| Total | 716 |

Table 2. Test results of YOLO-v7 models

| YOLO-v7 Model | mAP@50 | Precision | Recall | Model Summary | Per image Inference time (ms) |
|---------------|--------------|-------------|--------------|---|-------------------------------|
| YOLO-v7-tiny | 0.796 | 0.692 | 0.807 | 208 layers, 6015714 parameters, 13.0 GFLOPs | 3 |
| YOLO-v7 | 0.838 | 0.80 | 0.807 | 314 layers, 36497954 parameters, 6194944 gradients, 103.2 GFLOPs | 4.8 |
| YOLO-v7-x | 0.797 | 0.644 | 0.911 | 362 layers, 70802658 parameters, 0 gradients, 188.0 GFLOPs | 5.7 |

Table 3. Test results of YOLO-v8 models

| YOLO-v8 Model | mAP@50 | Precision | Recall | Model Summary | Per image Inference time (ms) |
|---------------|--------------|--------------|--------------|--|-------------------------------|
| YOLO-v8-n | 0.835 | 0.660 | 0.851 | 168 layers, 3006428 parameters, 8.1 GFLOPs | 3.1 |
| YOLO-v8-s | 0.800 | 0.684 | 0.760 | 168 layers, 11127132 parameters, 28.4 GFLOPs | 4.0 |
| YOLO-v8-m | 0.865 | 0.800 | 0.800 | 218 layers, 25842076 parameters, 78.7 GFLOPs | 5.8 |
| YOLO-v8-l | 0.811 | 0.700 | 0.833 | 268 layers, 43609692 parameters, 164.8 GFLOPs | 6.6 |
| YOLO-v8-x | 0.821 | 0.778 | 0.725 | 268 layers, 68127420 parameters, 0 gradients, 257.4 GFLOPs | 8.6 |

Table 4. YOLO-v7 test data performance

| Class | PR image | Precision | Recall | mAP@.5 |
|--------------|------------|--------------|--------------|--------------|
| Vertical | 31 | 0.676 | 0.742 | 0.711 |
| Mesioangular | 41 | 0.823 | 0.792 | 0.829 |
| Distoangular | 26 | 0.854 | 0.731 | 0.902 |
| Horizontal | 18 | 0.848 | 0.944 | 0.911 |
| All | 116 | 0.800 | 0.802 | 0.838 |

Table 5. YOLO-v8-m test data performance

| Class | PR | Precision | Recall | mAP@.5 |
|--------------|------------|--------------|--------------|--------------|
| Vertical | 31 | 0.693 | 0.774 | 0.799 |
| Mesioangular | 41 | 0.883 | 0.707 | 0.865 |
| Distoangular | 26 | 0.785 | 0.846 | 0.879 |
| Horizontal | 18 | 0.840 | 0.874 | 0.917 |
| All | 116 | 0.800 | 0.800 | 0.865 |

$$IoU = \frac{AreaBoundingBox(Ground\ Truth \cap Predicted)}{AreaBoundingBox(Ground\ Truth \cup Predicted)} \quad \text{Equation 1}^{13,21}$$

$$Precision = \frac{\#TP}{\#TP + \#FP} \quad \text{Equation 2}^{13,21}$$

$$Recall = \frac{\#TP}{\#TP + \#FN} \quad \text{Equation 3}^{13,21}$$

$$AP@threshold = \int p(r)dr \quad \text{Equation 4}^{13,21}$$

(area under the precision-recall curve)

$$mAP@threshold = \frac{1}{n} \sum_{i=1}^n AP_i \quad \text{for n classes} \quad \text{Equation 5}^{13,21}$$

Looking at the mAP metric values for all classes in the study, YOLO-v8-m performed better than YOLO-v7, with a difference of 2.7% (Figure 5). The precision-recall curve for the best model, YOLO-v8, is shown in Figure 7. Successful classifications for the proposed YOLO-v8-m model from the test data samples are presented in Figure 8, and the unsuccessful results are shown in Figure 9.

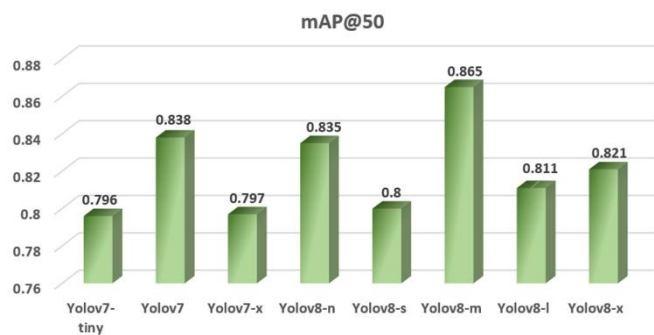


Figure 5. Performance analysis of YOLO-v7 and YOLO-v8 all model using the mAP metric.

The class-based performance comparisons of the best performing YOLO-v7 and YOLO-v8-m models on the test data are presented in Table 4 and Table 5. The “precision” and “recall” values for the four classes of YOLO-v7 are almost equal, 0.8 and 0.802, respectively, while for YOLO-v8-m, both values are 0.8. When comparing the precision metric across classes, the highest value for YOLO-v7 is 0.854 for the distoangular class, and for YOLO-v8-m, it is 0.883 for the mesioangular class. The lowest precision value is 0.676 for the vertical class in YOLO-v7 and 0.693 for YOLO-v8. When evaluating the recall metric across classes, the highest values are 0.944 for YOLO-v7 in the horizontal class and 0.874 for YOLO-v8-m in the same class. The lowest recall value is 0.731 for the distoangular class in YOLO-v7 and 0.707 for the mesioangular class in YOLO-v8-m.

AP@50

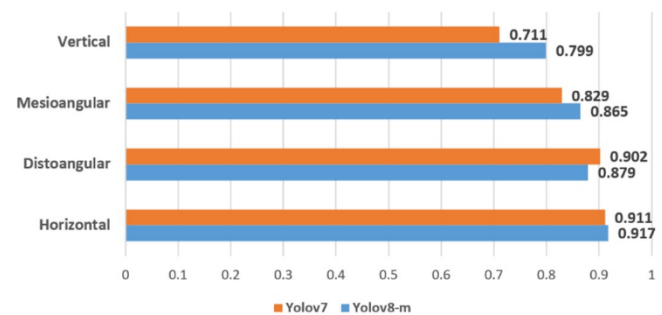


Figure 6. Performance analysis with the AP metric of best YOLO-v7 and YOLO-v8.

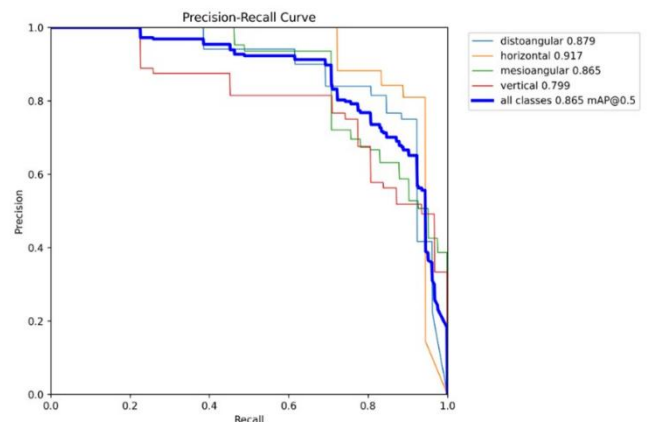


Figure 7. Performance analysis with Precision-Recall Curve for proposed model YOLO-v8-m.

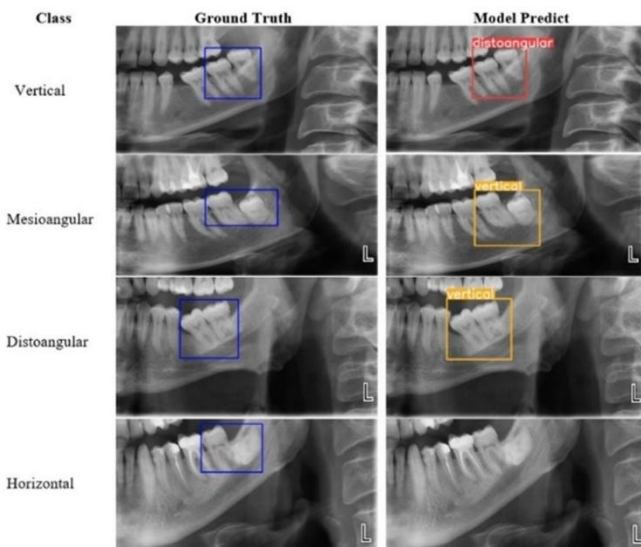


Figure 8. Example Winter classification true predict results for proposed model YOLO-v8-m.

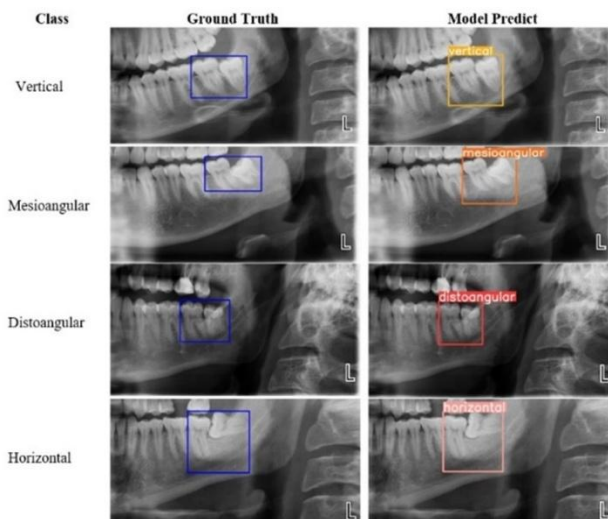


Figure 9. Example Winter classification results false predict results for proposed model YOLO-v8-m.

DISCUSSION

MITM are teeth that are often impacted and frequently require surgical extraction.²⁴ Dentists must proceed carefully when extracting these teeth to avoid harming the patient during and after the surgical procedure.¹² Radiological imaging is used to prevent or predict the likelihood of complications. The diagnosis made through classifications provides initial information about the likelihood of surgical complications.²⁵ PRs are the primary method for evaluating impacted tooth.²⁶ WC describes the impaction of the third molar in PRs and provides descriptive terms. It is also among the WC evaluation criteria to determine the positional relationship between the 2nd and 3rd molars based on the angle classification.

Yoo et al.¹⁴ presented a neural network model, ResNet-34, that can predict the extraction difficulty of MITM teeth. They evaluated the compatibility between their proposed model for 1053 MITM teeth, consisting of 600 PRs, and experts. They analysed the angular classification into four groups (mesioangular, distoangular, horizontal, and vertical positions) and assigned a score for each group. They reported that the correlation between the experts and the model in

angle classification was 90.23%. In our study, two AI models were used. While they used the Pederson Difficulty Score for angle classification; we used the WC classification.

Celik¹¹ proposed deep-learning models for WC in PR images. The study included 440 PR images with a total of 588 MITM teeth. Four models were presented: YOLOv3, ResNet50, AlexNet, and VGG16-based FASTER-RCNN. Among the models, YOLOv3 had the highest detection accuracy with a mAP@0.5 of 0.96. The study included a WC with only two classes: mesioangular and horizontal. In contrast, our study used a larger dataset and employed YOLO-v7 and YOLO-v8 models with convolutional neural networks to classify four types in WC.

Sukegawa et al.¹² proposed a model that performs both the Winter and Pell & Gregory classifications in PR images. The study examined 1330 MITM teeth in six groups: mesioangular, distoangular, horizontal, vertical, inverted, and buccoangular. After manually cropping the area, including the 2nd and 3rd molars in the PRs, the VGG16 neural network was used to classify the MITM teeth. They reported an accuracy of 86.63% for the WC. In their study, Maruta et al.¹³ evaluated the Winter and, Pell & Gregory classifications in similarly cropped PR images using the VGG16 algorithm. Their model performed with an accuracy of 79.59% on 1864 MITM teeth. Although we used a more limited dataset, possible reasons for obtaining better results compared to both studies may include our use of a WC with fewer classes and the application of multiple artificial intelligence models.

In studies which examined categories more than the current study, the region containing the WC information was cropped, and only the WC was determined.^{12,13} However, in our study, while determining the WC, the AI also identified where to focus on the PR images. Celik¹¹ performed object recognition on PR images; however, the WC was expanded from two categories to four categories (e.g., right and left), and only the third molar was examined. Since WC is determined based on the angulation between the second and third molars, WC localization in our study included both the second and third molars.^{12,13}

In this study, WC is addressed using the object recognition approach to determine the position of the second and third molars in PR images. Given the limited studies on this topic in the literature, the current study introduces an innovation by evaluating the second and third molars simultaneously as a four-class problem using state of the art of object recognition. Addition, the study presented an online angle measurement program as a practical method to measure the angle between the 2nd and 3rd molars.

Limitations of the study include:

- The relatively small amount of data,
- The inhomogeneous distribution of the data between classes, and
- The inability to investigate buccolingual and inverted positions due to the lack of data in the WC.

CONCLUSION

Our study presented YOLO-v7 and YOLO-v8 methods, which are CNN-based object recognition algorithms capable of performing WC in PRs. Radiological examinations before extraction contribute significantly to the surgical procedure. In this context, the automatic detection and classification of MITM teeth can reduce the time required for radiological diagnosis before the necessary treatments. An increase in the amount of data used, duplication of models for data augmentation, and additional studies on different AI models may be required.

Ethics Committee Approval: Ethics committee approval was obtained from Atatürk University Faculty of Dentistry Ethics Committee, Date: 20.01.2021/ Number: 04.

Informed Consent: This study was retrospective and only images from the radiology archive were used.

Peer-review: Externally peer-reviewed

Author Contributions: Concept – M.T.G., N.K., İ.Y.Ö.; Design – M.T.G., N.K., İ.Y.Ö.; Supervision – Ö.M., İ.Y.Ö., E.A.O.; Resources – M.T.G., Ö.M.; Materials – N.K., E.A.O.; Data Collection and/or Processing – M.T.G., N.K.; Analysis and/or Interpretation – Ö.M., İ.Y.Ö., E.A.O.; Literature Search – M.T.G., N.K.; Writing Manuscript – M.T.G., N.K., Ö.M.; Critical Review – Ö.M., İ.Y.Ö.

Conflict of Interest: The author of this article, Özkan Miloğlu, was also serving as a Section Editor of the journal at the time of submission. This situation constitutes a potential conflict of interest. In order to ensure an impartial and transparent peer-review process, the peer-review and publication decision for this manuscript were handled by a guest editor appointed by the Atatürk University Coordinatorship of Scientific Journals. A double-blind peer-review process was applied, and the author's editorial role was not disclosed to the reviewers. All stages of the evaluation process were conducted in accordance with the journal's ethical policies and international ethical guidelines, including those of COPE and ICMJE.

Financial Disclosure: This study was funded by grant FDK-2021-9758 from Ataturk University for Scientific Research Projects. We thank Ataturk University High-Performance Computing Application and Research Center IT for support.

Use of Artificial Intelligence: The authors declare that no generative artificial intelligence tools or large language models were used in the writing or editing of this manuscript.

Etik Komite Onayı: Atatürk Üniversitesi Diş Hekimliği Fakültesi Etik Kurulu'ndan 20.01.2021 tarihli ve 04 yıllık etik kurul onayı alınmıştır.

Hasta Onamı: Bu çalışma retrospektif olup sadece radyoloji arşivindeki görüntüler kullanılmıştır.

Hakem Değerlendirmesi: Diş bağımsız.

Yazar Katkıları: Konsept – M.T.G., N.K., İ.Y.Ö.; Tasarım – M.T.G., N.K., İ.Y.Ö.; Denetim – Ö.M., İ.Y.Ö., E.A.O.; Kaynaklar – M.T.G., Ö.M.; Malzemeler – N.K., E.A.O.; Veri Toplama ve/veya İşleme – M.T.G., N.K.; Analiz ve/veya Yorumlama – Ö.M., İ.Y.Ö., E.A.O.; Literatür Taraması – M.T.G., N.K.; Yazım Metni – M.T.G., N.K., Ö.M.; Eleştirel İnceleme – Ö.M., İ.Y.Ö.

Çıkar Çatışması: Bu makalenin yazarı Özkan Miloğlu, makale gönderildiği sırada derginin Bölüm Editörü olarak da görev yapmaktaydı. Bu durum potansiyel bir çıkar çatışması oluşturmaktadır. Tarafsız ve şeffaf bir hakem değerlendirme sürecini sağlamak amacıyla, bu makalenin hakem değerlendirmesi ve yayın kararı, Atatürk Üniversitesi Bilimsel Dergiler Koordinasyon Ofisi tarafından atanan bir konuk editör tarafından yürütülmüştür. Çift kör hakem değerlendirme süreci uygulanmış ve yazarın editörlük rolü hakemlere açıklanmamıştır. Değerlendirme sürecinin tüm aşamaları, derginin etik politikalarına ve COPE ve ICMJE dahil olmak üzere uluslararası etik yönergelerine uygun olarak gerçekleştirilmiştir.

Finansal Destek: Bu çalışma, Atatürk Üniversitesi Bilimsel Araştırma Projeleri Fonu'nun FDK-2021-9758 numaralı hibesiyle finanse edilmiştir. Atatürk Üniversitesi Yüksek Performanslı Hesaplama Uygulamaları ve Araştırma Merkezi BT'ye destekleri için teşekkür ederiz.

Yapay Zeka Kullanımı: Yazarlar, bu makalenin yazımı ve düzenlenmesi sürecinde herhangi bir üretken yapay zekâ aracı veya büyük dil modeli kullanılmadığını beyan ederler.

REFERENCES

- Roulias P, Kalantzis N, Doukaki D, Pachiou A, Karamesinis K, Damanakis G. Teeth eruption disorders: a critical review. *Children (Basel)*. 2022;9:771.
- Yamaguchi T, Hosomichi K, Shiota T, Miyamoto Y, Ono W, Ono N. Primary failure of tooth eruption: Etiology and management. *Jpn Dent Sci Rev*. 2022;58:258-267.
- Yıldırım H, Büyükgöze-Dindar M. Investigation of the prevalence of impacted third molars and the effects of eruption level and angulation on caries development by panoramic radiographs. *Med Oral Patol Oral Cir Bucal*. 2022;27:e106-112.
- Gümrükçü Z, Balaban E, Karabağ M. Is there a relationship between third-molar impaction types and the dimensional/angular measurement values of posterior mandible according to Pell & Gregory/Winter Classification? *Oral Radiol*. 2021;37:29-35.
- Santos KK, Lages FS, Maciel CAB, Glória JCR, Douglas-de-Oliveira DW. Prevalence of mandibular third molars according to the Pell & Gregory and Winter classifications. *J Maxillofac Oral Surg*. 2022;21:627-633.
- Shan T, Tay FR, Gu L. Application of artificial intelligence in dentistry. *J Dent Res*. 2021;100:232-244.
- Çelik B, Çelik ME. Automated detection of dental restorations using deep learning on panoramic radiographs. *Dentomaxillofac Radiol*. 2022;51:20220244.
- Nakamoto T, Taguchi A, Kakimoto N. Osteoporosis screening support system from panoramic radiographs using deep learning by convolutional neural network. *Dentomaxillofac Radiol*. 2022;51:20220135.
- Andrade KM, Silva BPM, de Oliveira LR, Cury PR. Automatic dental biofilm detection based on deep learning. *J Clin Periodontol*. 2023;50:571-581.
- Ha EG, Jeon KJ, Lee C, Kim HS, Han SS. Development of deep learning model and evaluation in real clinical practice of lingual mandibular bone depression (Stafne cyst) on panoramic radiographs. *Dentomaxillofac Radiol*. 2023;52:20220413.
- Celik ME. Deep learning based detection tool for impacted mandibular third molar teeth. *Diagnostics*. 2022;12:942.
- Sukegawa S, Matsuyama T, Tanaka F, et al. Evaluation of multi-task learning in deep learning-based positioning classification of mandibular third molars. *Sci Rep*. 2022;12:684-688.
- Maruta N, Morita K-i, Harazono Y, et al. Automatic machine learning-based classification of mandibular third molar impaction status. *J Oral Maxillofac Surg Med Pathol*. 2023;35:327-334.
- Yoo J-H, Yeom H-G, Shin W, et al. Deep learning based prediction of extraction difficulty for mandibular third molars. *Sci Rep*. 2021;11:1954.
- LabelImg. Version 1.4.0. PyPI. Accessed September 20, 2023. <https://pypi.org/project/labelimg/1.4.0/>
- Redmon J, Divvala S, Girshick R, Farhadi A. You only look once: unified, real-time object detection. In: Proceedings of the IEEE Conference on Computer Vision and Pattern Recognition; 2016:779-788.
- Jiang P, Ergu D, Liu F, Cai Y, Ma BJ. A review of Yolo algorithm developments. *Procedia Computer Sci*. 2022;199:1066-1073.
- Zhao H, Zhang H, Zhao Y. Yolov7-sea: Object detection of maritime UAV images based on improved Yolov7. In: Proceedings of the IEEE/CVF Winter Conference on Applications of Computer Vision; 2023:233-238.

19. Wang CY, Bochkovskiy A, Liao HYM. Yolov7: Trainable bag-of-freebies sets new state-of-the-art for real-time object detectors. In: Proceedings of the IEEE/CVF Conference on Computer Vision and Pattern Recognition; 2022:7464-7475.
20. Wu S, Li Z, Li S, Liu Q, Wu W. Static gesture recognition algorithm based on improved YOLOv5s. *Electronics*. 2023;12:596-601.
21. Jocher G, Chaurasia A, Qiu J. YOLO by Ultralytics. GitHub repository. Version 8.0.0. Accessed December 15, 2023. <https://github.com/ultralytics/ultralytics>.
22. Common Object in Context. Accessed December 29, 2023. <https://cocodataset.org/#home>.
23. Diwan T, Anirudh G, Tembhurne JV. Object detection using YOLO: Challenges, architectural successors, datasets and applications. *Multimed Tools Appl*. 2023;82:9243-9275.
24. Issrani R, Prabhu N, Sghaireen M, et al. Comparison of digital OPG and CBCT in assessment of risk factors associated with inferior nerve injury during mandibular third molar surgery. *Diagnostics*. 2021;11:2282.
25. Ishii S, Abe S, Moro A, Yokomizo N, Kobayashi Y. The horizontal inclination angle is associated with the risk of inferior alveolar nerve injury during the extraction of mandibular third molars. *Int J Oral Maxillofac Surg*. 2017;46:1626-1634.
26. Ghai S, Choudhury SJ. Role of panoramic imaging and cone beam CT for assessment of inferior alveolar nerve exposure and subsequent paresthesia following removal of impacted mandibular third molar. *J Oral Maxillofac Surg*. 2018;17:242-247.